Available online at www.sciencedirect.com
ScienceDirect
International Journal of Mass Spectrometry 270 (2008) 52–61
International Journal of Mass Spectrometry
www.elsevier.com/locate/ijms

Nonspiked ^{40}Ar and ^{36}Ar quantification using a quadrupole mass spectrometer: A potential for K–Ar geochronology

Virgile Rouchon *, Jean-Claude Lefèvre, Xavier Quidelleur, Gilles Guérin, Pierre-Yves Gillot

Universite Paris Sud, Laboratoire de Geochronologie Multi-Techniques, CNRS UMR-IDES 8148, Departement des Sciences de la Terre, Bat. 504, 91405 Orsay Cedex, France

Received 10 October 2007; received in revised form 23 November 2007; accepted 26 November 2007
Available online 4 December 2007

Abstract

Potassium–argon geochronology relies on the absolute quantification of radiogenic ^{40}Ar (^{40}Ar*) produced by the natural decay of ^{40}K in K-bearing rocks and minerals. It implies the precise determination of the ^{40}Ar and ^{36}Ar contents to account for atmospheric contamination, which, for very young (<100 kA) and/or K-poor material (K < 0.2 wt.%), may represent over 99% of their argon budget. We have tested the applicability of a standard resolution quadrupole mass spectrometer (QMS) for the determination of ^{40}Ar* in a set of K–Ar and ^{40}Ar/^{39}Ar international geochronological standards.

The analytical apparatus is designed to perform in-line extraction, purification and measurement of 10^{12} to 10^{14} atoms of Ar from various K-bearing minerals. The sensitivity of the mass spectrometer is calibrated against the international K–Ar standard GL-O and determined with a 0.6% (1σ) uncertainty. The average ^{40}Ar/^{36}Ar ratio of repeated air-standards through a 1-month period is 262.5 ± 0.36 (1σ), and its daily standard deviation never exceeds 1‰.

Geochronological standards MMhb-1 (520.4 ± 1.7 Ma, hornblende), LP-6 (127.8 ± 1.4 Ma, biotite), Taylor Creek Rhyolite (27.92 ± 0.04 Ma, TCR sanidine), Alder Creek Rhyolite (1.193 ± 0.001 Ma RAC-20 sanidine) and RMF96 (0.331 ± 0.002 Ma, sanidine) dated here at 529.7 ± 7.2, 130.1 ± 1.0, 29.13 ± 0.4, 1.189 ± 0.022 and 0.340 ± 0.006 Ma, respectively, are within or close to their published reference ages at the 1σ confidence level.

Recent high-sensitivity and high-resolution quadrupole mass filters, equipped with appropriate and high stability electronic equipments, provide compact and fast analytical alternatives to expensive magnetic-sector-type mass spectrometers for applications such as K–Ar geochronology.

Keywords: Quadrupole mass spectrometer; K–Ar geochronology; Volcanism; Geochronological standard

1. Introduction

K–Ar geochronology is an absolute rock-dating method based on the natural radioactive decay of ^{40}K to ^{40}Ar*. The independent measurement of ^{40}Ar, ^{36}Ar and ^{40}K in an adequate mineral phase allows determining the time of closure of the K–Ar geochronometer, which may characterize the time of emplacement of magmatic rocks or the timing of a thermal metamorphic event. The particularity of the K–Ar method is that it may be applied to the whole history of the Earth, thanks to the long half-life of ^{40}K (1.25 billions years) and its abundance as a major element in common minerals of the Earth's crust, allowing detectable amounts of ^{40}Ar* to be accumulated in relatively short amounts of time (i.e., several thousands of years). Two different K–Ar techniques are in use. The conventional technique relies on the measurement of a mixture between a precisely known ^{38}Ar spike and the sample to be dated. Such an approach requires the measurement of isotopic ratios only (^{40}Ar/^{38}Ar and ^{36}Ar/^{38}Ar). The alternative technique, the Cassignol–Gillot [1] or nonspiked technique, relies on very stable mass spectrometer (MS) conditions for direct quantification of ^{40}Ar and ^{36}Ar content, making the ^{38}Ar spike unnecessary. Within the last two decades, we have acquired a strong expertise in building our own instruments for both K–Ar [2] and ^{40}Ar/^{39}Ar [3] dating techniques, and have demonstrated that the former technique is suitable over a wide geological time interval, from Mesozoic to

* Corresponding author. Tel.: +33 1 69 15 48 93; fax: +33 1 69 15 48 91.
E-mail address: virgile.rouchon@u-psud.fr (V. Rouchon).

1387-3806/$ – see front matter © 2007 Elsevier B.V. All rights reserved.
doi:10.1016/j.ijms.2007.11.009

Holocene (e.g., [4–8]), extended to the historical period [2,9]. However, the hypothesis that the K–Ar chronometer remained closed in rocks and minerals can be erroneous. Indeed, K may be exchanged during fluid–rock interactions, while heating in geological environments (for example at temperature above 250 °C for K-feldspar [10]) may cause Ar to escape by diffusion. Because the K–Ar technique does not allow to check *in fine* that the chronometer remained closed, it is mandatory to apply a severe sample selection and preparation in order to avoid disturbed rocks and minerals. Unfortunately, due to improper sample selection made in the past, the K–Ar technique now suffers from an outdated bad reputation. The $^{40}Ar/^{39}Ar$ dating technique, which also relies on the radioactive decay of ^{40}K to ^{40}Ar, has been extensively developed as an alternative (see [10], for a complete description of this technique). With the $^{40}Ar/^{39}Ar$ technique, ^{39}K is converted to ^{39}Ar by a neutron flux in a nuclear reactor in order to use ^{39}Ar as a proxy for the determination of ^{40}K. After irradiation, the measurement by mass spectrometry of the $^{36}Ar/^{39}Ar$, $^{37}Ar/^{39}Ar$, $^{38}Ar/^{39}Ar$ and $^{40}Ar/^{39}Ar$ ratios of a given sample gas fraction is therefore sufficient to determine a radiometric age. The main advantage of the $^{40}Ar/^{39}Ar$ technique lies in the stepwise heating approach, which allows the identification of thermally disturbed samples. However, the $^{40}Ar/^{39}Ar$ technique is limited by several drawbacks such as ^{39}Ar recoil effects during irradiation of fine-grained samples, and production of interference Ar isotopes, mainly from Ca, which may affect age determinations for samples with low K/Ca ratios, such as basalts and andesites for instance. In addition, the $^{40}Ar/^{39}Ar$ technique relies on primary age standards for neutron flux calibration, which are dated by the K–Ar technique. It then appears to us that improving K–Ar dating remains an up to date objective. Therefore, we have undertaken the development of a low-cost, maintenance-easy facility for K–Ar geochronology using a quadrupole mass spectrometer for precise Ar isotopic measurements. The use of this type of mass spectrometer for both the K–Ar and $^{40}Ar/^{39}Ar$ techniques has not been reported yet.

Quadrupole mass spectrometers (QMSs) are used in a wide variety of industrial and research applications from qualitative analytical chemistry to high-end isotopic analyses. They are produced on an industrial scale by laboratory equipment companies as specific task-dedicated analytical tools such as gas chromatography–mass spectrometric (GC–MS) systems, as inductively coupled plasma–mass spectrometric (ICP–MS) systems, or as simple residual-gas characterization and leak-detectors in vacuum lines. Custom-made QMS systems are available for non-ubiquitous applications, allowing the adaptation of this analytical tool to specific scientific purposes (e.g., [11]), taking advantage of the low-cost and robustness of industrially produced equipment.

Laboratory-adapted quadrupole mass spectrometers (QMS) have been used in Earth Sciences to measure elemental and isotopic composition of noble gases [12,13] and nitrogen [14,15], using both spike [13] and nonspike methods [11]. To measure these gaseous species at nano- to pico-mole levels, QMS commonly use electron multiplier (EM) ion-detectors, which, unfortunately, are generally considered as having unstable current outputs. For this reason, QMS–EMs are mainly used to analyze mass ratios, and precise quantification is achieved only by spike methods (e.g., [12,13]) or isotope dilution [16]. However, pressure calibration of QMS–EM sensitivity enabled quantitative measurements of nano-mole quantities of N_2 and Ar ($\pm 5\%$ at 2σ [17]), demonstrating the ability of QMS–EM for the nonspiked quantification of small amounts of gas. We present here the first application of a QMS–EM for nonspiked quantitative Ar and $^{40}Ar/^{36}Ar$ measurements in minerals, calibrated and validated against several international geochronological standards.

2. Experimental materials and methods

2.1. High-vacuum line design

The facility design allows in-line extraction, purification, calibration and isotopic measurement of argon from a rock or a mineral phase (Fig. 1). Stainless steel line parts and valves are assembled with copper gaskets to ensure ultra-high vacuum. A pressure below 10^{-8} Torr (1.3 μPa) is achieved by using two turbomolecular pumping units and monitored by cold and hot cathode ionization gauges (Fig. 1). Four units in the gas line can be distinguished which are, in gas processing order, the extraction unit (E), the condensable gas purification unit (P1) the non-condensable gas purification unit (P2), the standard and calibration unit (STD) and the spectrometric unit (Sp).

In the E unit, gas extraction is performed using a 3000 W radio-frequency induction furnace. The heating electrical conductor is a molybdenum crucible positioned at the bottom of a single-envelope quartz tube cooled by a room temperature water flow. Temperatures above 1600 °C (1873 K), sufficient to melt any silicate mineral phase, are routinely reached with this furnace.

Purification of condensable gas is achieved in the P1 unit by using a CuO–Cu/cold-trap couple. Cu–CuO heated at 650 °C (923 K) oxidizes reduced carbon and hydrogen species to H_2O and CO_2, which are then condensed on the cold-trap (CGT, Fig. 1) consisting of a pyrex tube cooled at a temperature just above the boiling point of nitrogen. This apparatus also condenses any chlorine compounds, source of isobaric interference at mass 36 ($^1H^{35}Cl$), that would be degassed from the sample. The pressure in the P1 unit is monitored with a Granville–Philips convectron gauge (CG, Fig. 1) from atmosphere down to 10^{-4} Torr (13 mPa) in order to control the status of the purification process.

The P2 unit is used to purify remaining gaseous species (N_2 and traces of hydrocarbons) on Ti-foam heated at 750 °C (1023 K). An activated charcoal cold finger (CT, Fig. 1), at liquid nitrogen temperature, is used to concentrate the total gas yield into the P2 unit to isolate the rest of the line from the extraction-contaminated E–P1 units before further gas processing.

The STD unit is used to insert calibrated gas standard (atmospheric Ar) in the spectrometric unit. The standard gas is stored in a ~1 l stainless steel tank from which 1 ± 0.01 ml is pipetted and introduced into the spectrometric unit (Fig. 1). A 200 °C

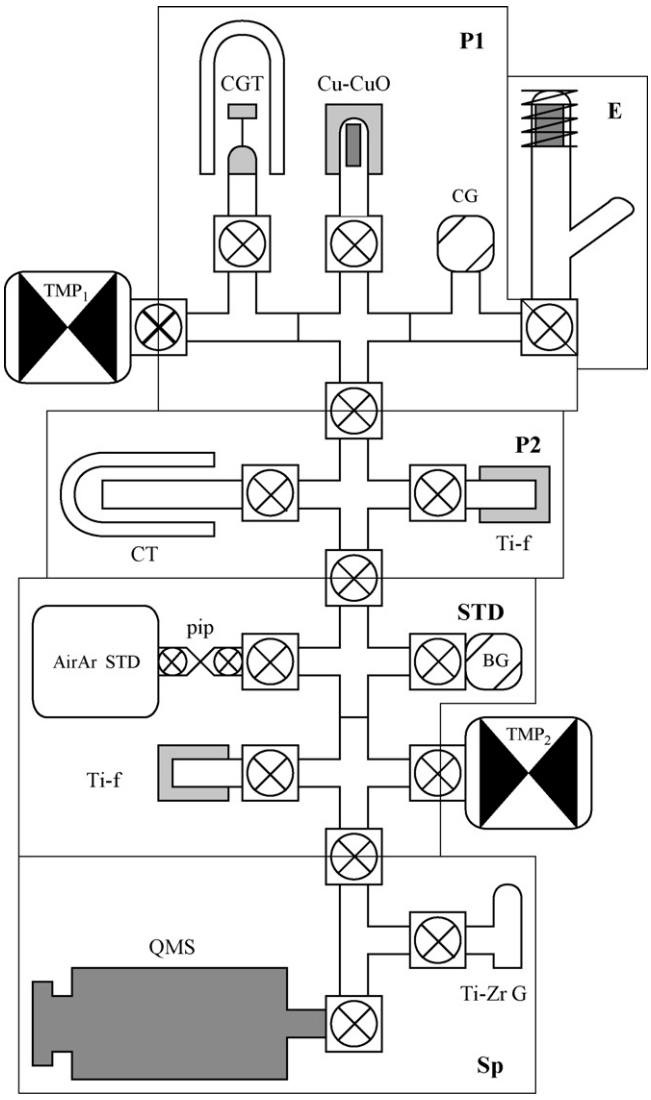

Fig. 1. Schematic description of the high-vacuum line. E: extraction unit; P1: condensable gas purification unit; P2: non-condensable gas purification unit; STD: standard calibration unit; Sp: spectrometer unit; CG: convectron gauge; Cu–CuO: copper–copper oxide; CGT: condensable gas-trap; TMP: turbo molecular pump; CT: cold-trap; Ti-f: titanium foam; BG: Baratron gauge; Ti–Zr G: titanium zircon getter pump; QMS: quadrupole mass spectrometer.

(473 K) Ti-foam finger is used to purify hydrogen and trace impurities remaining in the sample and standard gas before their introduction in the spectrometer. The STD unit is equipped with a 20 mTorr Baratron gauge (BG, Fig. 1) to monitor the gas pressure from samples, avoiding the introduction of over range amounts of gas in the spectrometric unit. A Ti–Zr getter at a temperature of 400 °C (673 K) continuously purifies the Sp unit (Fig. 1).

2.2. Quadrupole mass spectrometer hardware

The spectrometer used was developed from an SXP Elite system by VG (Fisons Instruments, purchased in 1994). Due to our specific requirements, parts of the original electronic devices were replaced.

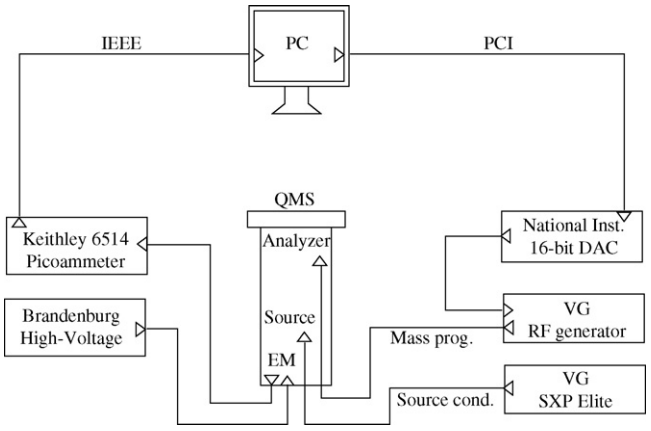

Fig. 2. Hardware configuration of the spectrometer.

The QMS is composed of an electron-impact ionization source equipped with a thoriated iridium filament. The ions are accelerated and admitted to the analyzer by an ion extractor. The analyzer (VG AN-9N) is 262-mm long and 56-mm wide, composed of four 12-mm diameter cylindrical molybdenum electrodes. Ion detection is achieved by a Faraday-cup or by an electron multiplier (EM). The total volume of the mass spectrometer recipient is approximately 1 l.

The default VG radio-frequency generator was adjusted at the factory for measurements in the mass/charge (*N*/*Z*) range 0–50. A resolution parameter defines the peak width over the entire mass range, providing a ^{40}Ar mass contribution at mass 39 of less than 10^{-4} at an intermediate resolution ($\Delta m/m = 70$ at mass 40). The 4 amu difference between ^{36}Ar and ^{40}Ar allows to work with a poor resolution setting, resulting in a higher sensitivity of the system. The direct voltage applied to the electrodes (in the range 0–10 V) controls the analyzed *N*/*Z* value. A 16-bit National Instrument (−10/+10 V output) DAC provides this voltage (Fig. 2), allowing a good stability of the analyzer during multiple ion monitoring and an improved precision during peak scanning (scan increment = $1.5 \times 10^{-3} \pm 0.5$ amu/step, Fig. 3), allowing the fine selection of the peak-top tension (Fig. 3).

The source conditions are controlled by the original VG SXP-Elite electronics (Fig. 2). A trap-current control of 0.3 mA regulates the electron production. The Ar ionization efficiency was observed to be optimum at an electron energy setting of 47 eV, minimizing double ionization effects. The extractor voltage (0–100 V) was set to 25.3 V with a pole bias of 20 V, for which the peak shape was optimum (Fig. 3). Although not symmetrical and perfectly flat, the best peak we were able to obtain is characterized by a flat section at its top, covering a sufficient mass range for the signal to be stable given the precision of the direct voltage applied to the mass filter (Fig. 3).

Ion detection is achieved using an electron multiplier (EM) in order to reach the required sensitivity for precise ^{40}Ar and ^{36}Ar measurements. The EM high voltage (HV = 1700 V) was driven by a Brandenburg 477 HV generator; with a precision better then 15 ppm during a routine measurement run (Fig. 2). The output of the EM was measured by a Keithley 6514 picoammeter with an internal noise below 10^{-16} A. One of the advantages of the QMS being the rapidity and stability of peak-to-peak jumps

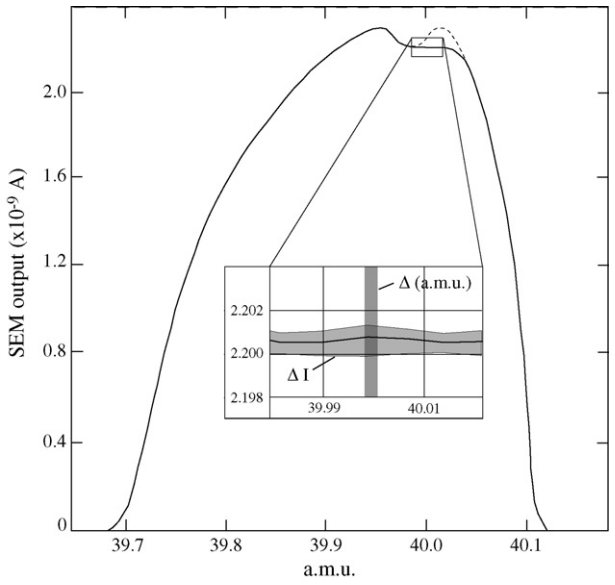

Fig. 3. Peak scan at mass 40 in standard analytical conditions. The dashed line corresponds to the peak shape in inadequate pole-bias and ion extractor conditions. The box represents the flat portion of the peak, where the peak height is measured to achieve quantification. Δ (amu) is the precision of the direct voltage applied to the mass filter and is of 1.5×10^{-3} amu, ΔI is the noise level of the SEM output, typically below 0.05%.

during multiple ion monitoring, the quality of this electrometer was critical to minimize single measurement time, in order to increase the number of measurements within each analysis procedure.

The mass filter and the detector were controlled and monitored with the National Instrument Labview platform by a program specifically developed for our analytical system.

2.3. Mass spectrometry measurement procedure

The main drawback of the QMS was the high retention of a gas fraction introduced, resulting in a large memory effect. The large volume and the numerous isolating ceramics provide an important adsorptive surface, leading to extensive elemental and isotopic exchanges between adsorbed and gaseous Ar. Consequently, the static rise or drop rates of the QMS were high when sample gases with pressure differences of more than one order of magnitude were measured sequentially (Fig. 3a). In order to minimize these effects, the QMS measurement chamber, when not measuring, was systematically put in equilibrium with an atmospheric air pipette, specifically prepared to be in the pressure range expected for samples to be measured (a function of known K contents and rough age estimates). This ensured that sorption/desorption effects did not produce more than 1% variation of the ^{40}Ar signal, correctly approximated by a linear function of time throughout the analysis (500 s). This method also allows to accurately correct for desorption by the atmospheric contamination correction, because desorbed gas have an atmospheric isotopic ratio. However, important differences between atmospheric and sample ^{40}Ar/^{36}Ar ratios may lead to a variability of several percents at mass 36, like for the glauconite K–Ar standard GL-O (Fig. 4b). Whereas the ^{40}Ar current of the GL-O is essentially stable (<0.5‰ variation) throughout the measurement procedure, ^{36}Ar increases by 10% as a response to the high ^{40}Ar/^{36}Ar ratio of the GL-O and its equilibration with adsorbed Ar of atmospheric composition.

Ion implantation in the electron multiplier (EM) and at the source caused a significant sensitivity decrease during measurements in the pressure range $(5–1) \times 10^{-6}$ Torr (0.7–0.12 mPa). At the highest pressure in this range, the sensitivity linearly decreased by 2% during a single analysis (Fig. 4c). The initial sensitivity could be recovered in 24 h implying no specific damaging or implantation-related aging of the EM.

The output of the EM installed in the QMS requires a significant time to stabilize to the ^{40}Ar ion beam, which results in an increase of the output current as an inverse function of time (Fig. 4d). An important equilibration time was therefore necessary to reach a status where the evolution of the output current becomes independent of EM sensitivity variations. The equilibration time is a direct function of the ^{40}Ar signal, and is therefore minimized at higher Ar pressures. The equilibration procedure employed consists of a prolonged transmission of ^{40}Ar ions to the EM until its output stabilizes (typically 100 s), and before the measurements of ^{40}Ar and ^{36}Ar are started.

The successive measurements at masses 40 and 36 during an analysis procedure were regressed to the time of sample introduction (t_0) to account for the sorption/desorption and implantation effects, with EM equilibration effects removed. These t_0 values of masses 40 and 36 were used to determine the total Ar yield and the ^{40}Ar/ ^{36}Ar ratio (Fig. 5).

2.4. Rock-dating analytical procedure

Before initiating a measurement procedure, the line vacuum is checked to be below 10^{-7} Torr on a Bayard–Alpert gauge (P2). The Cu–CuO is heated up from 450 °C (723 K) to 650 °C (923 K) and pumped by the TMP_1. When this temperature is reached, the STD/P_2, P_2/P_1 and P_1/TMP_1 valves are closed to set the E–P_1 volumes in static mode. The extraction and condensable-gas purification is done synchronously with the E/P_1 valve open and E–P_1 volume isolated from the rest of the line. The CGT is cooled down to −180 °C (93 K).

Sample heating is done incrementally with 0.1 A steps of inductive current. At each heating step, the pressure in P_1 first increases and then decreases as a result of sample degassing and purification. The intensity is increased only when the pressure in E–P_1 drops below 10^{-2} Torr (monitored on CG). This prevents damage to the crucible by the interaction of reactive gases with Mo at high temperature. Six to seven steps are required depending on the temperature to reach for complete gas extraction from the sample (Tf, hereafter). Tf is maintained during the time required for sufficient purification ($P < 10^{-4}$ Torr or 12 mPa), after which the gas is expanded to P_2 and absorbed on CT for 15 min. After reaching to CT, the temperature of the sample (E) is slowly decreased to ambient temperature and the CT valve is closed. The rest of the E–P_1–P_2 units is pumped by the TMP_1 and background pressure is checked on the cold cath-

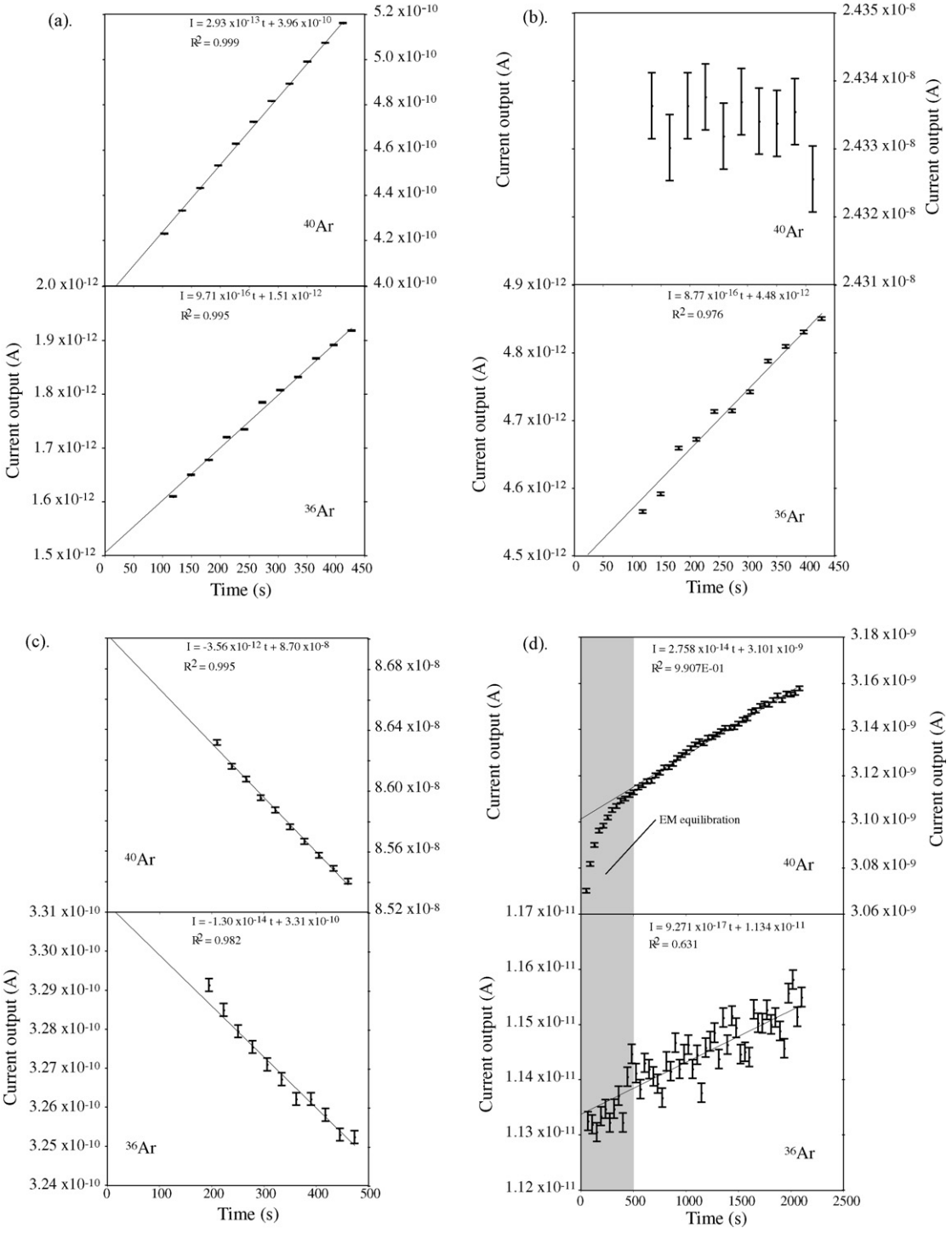

Fig. 4. Mass spectrometer signal evolution with time as a function of (a) degassing of adsorbed Ar during a line blank measurement after QMS equilibrium with an air-standard pipette; (b) degassing of ^{36}Ar during a GL-O sample measurement with a similar pressure to an air-standard pipette; (c) signal decrease due to ion implantation on the EM at higher Ar pressure (here 4×10^{-6} Torr in the Sp unit); and (d) signal increase due to electron multiplier equilibration. Only the first 500 s of the signal increase are here attributed to EM equilibration. The linear tendency is due to surface degassing of adsorbed Ar. All signal values are SEM outputs. For each point, ^{36}Ar is determined by averaging 20 s of continuous SEM output, while ^{40}Ar is determined by averaging 10 s of continuous SEM output. Error bars represent 1σ uncertainties of the SEM output during this measurement time.

ode gauge (not exceeding 5×10^{-7} Torr or 0.7 μPa in standard conditions).

The P_1/P_2 valve is closed and the gas sample is expanded to P_2 and left 30 min to purify on the P_2 Ti-f. The Ti-f temperature is then decreased below 400 °C (673 K) to ambient temperature to allow hydrogen to be retained by the titanium foam. The gas sample is then expanded to STD where its pressure is checked not to exceed 2×10^{-5} Torr (2.7 mPa) on the Baratron gauge.

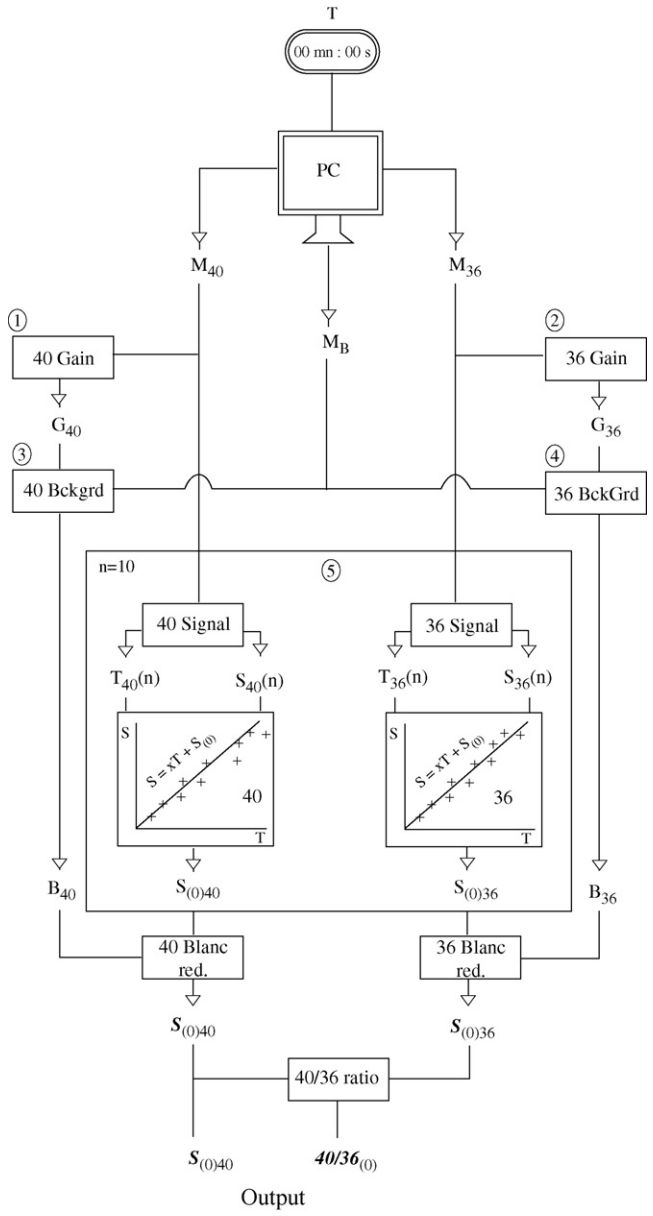

Fig. 5. Schematics of the QMS measurement procedure as developed using the Labview platform. Mass programs M_{40} and M_{36} are fed to the analyzer via the PC interface. (1 and 2) Gain identification; (3 and 4) background measurements; (5) sequence of 10 measurement cycles at masses 40 and 36. The data is processed for time regression and background correction.

The gas is left 5 mn on the STD Ti-f to ensure purification of any residual impurities.

The gas is then expanded to Sp where the spectrometric analysis is initiated. After EM equilibration and background measurements, the gas is isotopically equilibrated and the Sp/STD valve is closed for the sequential measurements of masses 40 and 36 (Fig. 5). After the sample analysis, the sample gas is pumped out by TMP_2. A calibrated air pipette is expanded to P_2 and STD. It is left 5 min to purify on STD Ti-f and then expanded to Sp where it is analyzed in the same conditions as the sample gas, providing a direct calibration of the QMS sensitivity.

The atmospheric contamination correction is performed by measuring a second pipette of the air standard immediately after

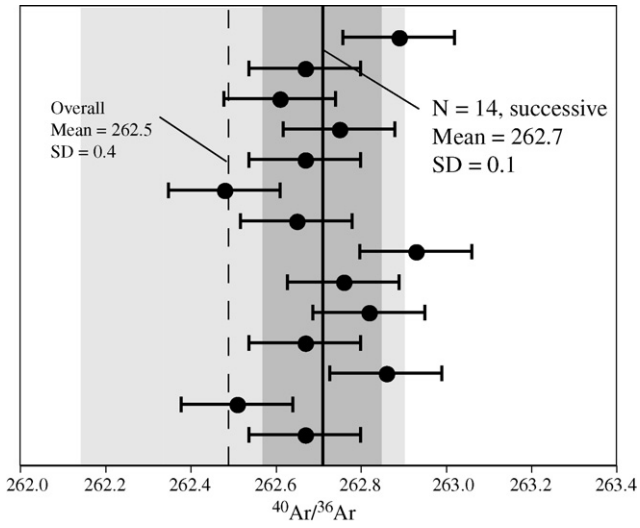

Fig. 6. (a) Mass spectrometer sensitivity vs. $^{40}Ar/^{36}Ar$ deviation from mean atmospheric value of individual air pipettes during a 1-month period and (b) $^{40}Ar/^{36}Ar$ ratio of 14 successive individual air-standard pipette measurements.

the sample analysis, in the same Ar pressure conditions as the sample. The correction is based on the hypothesis that all of the non-radiogenic Ar contained in the sample has an atmospheric isotopic composition [2,9]. If the isotopic ratio of air ($R_{atm} = {}^{40}Ar/{}^{36}Ar$) is measured in the same analytical and pressure conditions as the sample, atmospheric ^{40}Ar ($^{40}Ar_{atm}$) can be calculated as

$$^{40}Ar_{atm} = {}^{36}Ar \times R_{atm}$$

This approach directly takes into account the pressure dependence of the isotopic ratio, which results from the pressure dependence of the mass dependent fractionation in the QMS.

3. Results and discussion

3.1. Performance of the mass spectrometer

The ^{40}Ar and ^{36}Ar signals of atmospheric Ar pipettes from an air-standard tank ($V = 1$ l, $P = 9.4 \times 10^{-3}$ Torr or 1.25 Pa, n ($^{40}Ar^*$) $= 2.32 \times 10^{14}$ at./pipette) were measured several times daily over a period of 1 month for QMS sensitivity calibration. The ^{40}Ar sensitivity in the measurement conditions defined above is of 4.29×10^{-22} A/at., corresponding to a pressure of $\sim 2 \times 10^{-6}$ Torr (0.27 mPa) in the Sp volume (Fig. 1). The atmospheric $^{40}Ar/^{36}Ar$ isotopic ratio measured is 262.5 with a monthly standard deviation of 0.36 (0.14%). The difference to the reference value of $^{40}Ar/^{36}Ar_{atm} = 295.5$ [18] is due to the mass discrimination in the ion source, in the analyzer and the ion detection system, all contributing to the mass dependence of the QMS sensitivity. Within stable source, EM and analyzer conditions, successive measurements of 14 independent pipettes resulted in a standard deviation of the $^{40}Ar/^{36}Ar$ ratio of less than 0.06% (262.71 ± 0.13, Fig. 6).

At a pressure of 3.5×10^{-8} Torr (4.6 μPa), the analytical uncertainty on the ^{36}Ar measurement increases to 0.25% while ^{40}Ar remains measured with uncertainties below 0.06%. This results in a poor stability of the $^{40}Ar/^{36}Ar$ ratio in this lower

range of Ar pressures. The best analytical error on the determination of the $^{40}Ar/^{36}Ar$ ratio is achieved at the upper half of the studied pressure range and is typically of 0.06% (1σ), mainly imposed by the uncertainty on the measurement of ^{36}Ar (0.05%), which is 2–4 times higher than the uncertainty on ^{40}Ar. The weight of samples to be dated consequently needs to be adjusted to provide Ar pressures in the range 2×10^{-6} to 2×10^{-7} Torr (0.27–0.027 mPa or $\sim 10^{13}$ at. $^{40}Ar^*$) in the Sp unit. This range is a good compromise between the limitation of ion implantation in the EM and the maximizing of the signal. It is also critical to consider uncertainties from external factors, like weighting of the sample, which, for K-rich and very radiogenic samples, may become important when minimizing the pressure of Ar for measurement. For example, the higher pressures in the range adopted for our analytical procedure correspond to 10 mg of Archean-Paleo-Proterozoic samples with a K content of 8 wt.%, a lower limit for a mass determination requirement better than 0.5%.

Hot and cold line blanks of the complete sample analytical procedure were measured frequently to ensure that the contribution of the line to atmospheric contamination is limited and correctly accounted for. The typical hot line blank ^{40}Ar contribution is of (1–10) $\times 10^{11}$ atoms with $^{40}Ar^*$ proportions of 0.0 ± 0.1% (Table 1), confirming the accuracy of our atmospheric contamination correction. No significant isotopic fractionation is thus observed during temperature increments up to 1600 °C. Cold blanks have very low Ar yields (4.0×10^{10} at.) with sub-atmospheric $^{40}Ar/^{36}Ar$ ratios ($^{40}Ar^* = -18$%, Table 1), suggesting kinetic fractionation of minute air-leaks in the line at ambient temperature. However, this Ar yield represents below 1‰ of the typical sample yield and therefore creates no detectable disturbance associated with atmospheric contamination correction.

3.2. Sensitivity calibration and dating performances

Calibration of the air standard was achieved using the GL-O international standard [19]. The procedure described above was performed with GL-O aliquots of 50–100 mg (Table 1).

Table 1
K–Ar dating of international standards

Sample	Weight (g)	$^{40}Ar^*$ (%)	^{40}Ar ($\times 10^{13}$ at.)	$^{40}Ar^*$ ($\times 10^{14}$ at./g)	K (%)	Age (Ma)	Uncert. (Ma)
	0.0643	94.18	4.57	6.698	6.55	94.52	1.3
	0.0695	93.11	5.00	6.705	6.55	94.55	1.3
	0.0754	94.57	5.34	6.701	6.55	95.34	1.3
	0.0714	94.20	5.06	6.677	6.55	95.44	1.3
GL-	0.0828	95.47	5.79	6.671	6.55	95.38	1.3
O	0.0609	93.50	4.35	6.682	6.55	95.05	1.3
	0.0835	95.14	5.90	6.723	6.55	94.97	1.3
	0.0955	87.26	7.27	6.638	6.55	95.12	1.3
	0.0676	86.88	5.17	6.641	6.55	95.69	1.3
	0.0761	92.30	5.45	6.611	6.55	94.14	1.3
Mean						95.0	0.5/1.0
Ref. [19]				6.68		95.0	1.1
MMhb-1	0.0293	98.2	2.99	10.03	1.56	529.7	7.2
Ref. [22]				9.80		525.1	2.3
	0.0621	92.1	7.94	11.781	8.37	130.0	1.8
LP6	0.1346	94.2	16.7	11.757	”	129.7	1.8
	0.0485	97.1	5.90	11.832	”	130.5	1.8
Mean						130.1	1.0/1.3
Ref. [19]				11.58		127.8	0.7
TCR2	0.0641	69.4	1.99	2.164	7.06	29.13	0.40
Ref. [22]						28.34	0.16
RAC-20	0.2404	16.4	1.60	0.1098	8.84	1.189	0.022
Ref. [28]						1.193	0.001
RMF96	1.0025	17.8	2.18	0.0390	10.99	0.340	0.006
Ref. [30]						0.331	0.002
Hot blank		−0.08	0.0918				
Hot blank		−0.02	0.0922				
Cold blank		−17.7	0.0040				

RMF96 [30], RAC-20 [28], TCR-2 [22], LP-6 [19] and MMhb-1 [21] are calibrated against the GL-O [19]. Individual GL-O data given as calibrated against all other GL-O measurements (see Fig. 6). Most recently proposed reference values for each standard are given. Line blank measurements are shown as an indication of the accuracy of the atmospheric contamination correction. $^{40}Ar^*$: radiogenic argon; uncert.: age uncertainty at the 1σ level; mean: weighted (by $1/\sigma^2$ [31]) mean age and associated uncertainty/1% uncertainty, which we consider as minimum. Ages were obtained using ^{40}K decay constants and K isotopic ratios of [18].

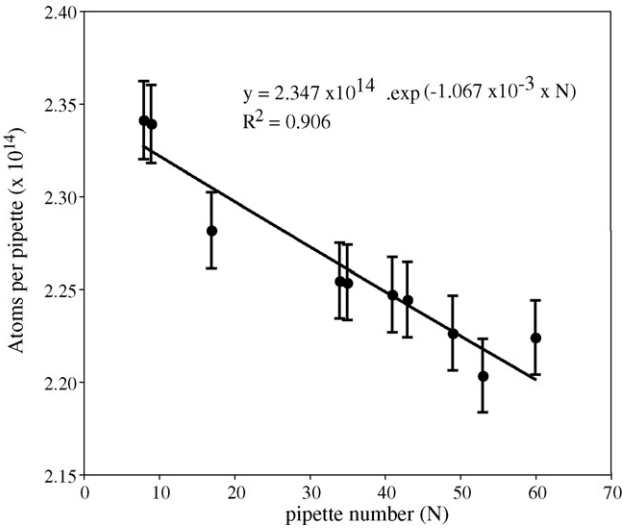

Fig. 7. Calibration of the air-standard tank by measurement of the GL-O K–Ar standard [19]. Each point represents the number of atoms per pipette volume of successive pipette measurements, based on calibration by using aliquots of the GL-O standard. Error bars correspond to the uncertainty on the ^{40}Ar* content of the GL-O (1%). The exponential fit represents the decrease of the pressure in the standard tank by successive pipetting.

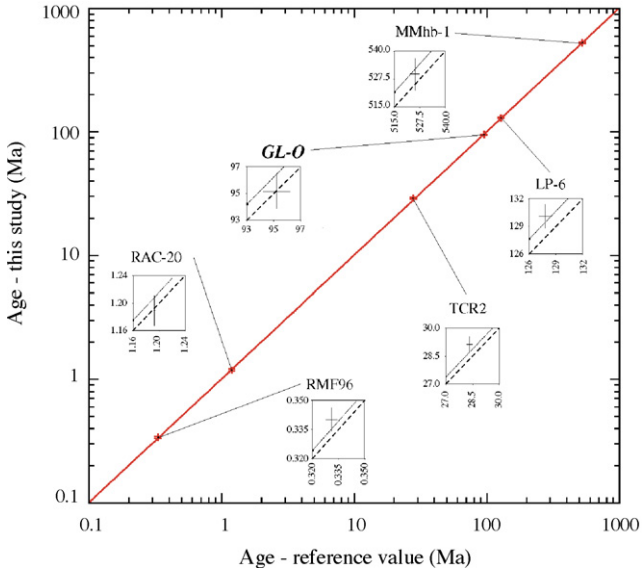

Fig. 8. Direct comparison of reference ages with ages determined in this study for the various geochronological standards analyzed (Table 1). The least square fit of the data points is given (solid line), in comparison with the slope 1 line (dashed line).

The ^{40}Ar* content of the GL-O ($6.68 \pm 0.06 \times 10^{14}$ at./g [19]) was used to determine the signal over yield sensitivity (A/at.) of our system. Each GL-O measurement was immediately followed by the measurement of a single air-standard pipette from the standard tank, thereby determining the total ^{40}Ar amount in the pipette. Multiple single pipette calibration allowed us to determine the ^{40}Ar decrease of the standard tank (see Fig. 1), thereby also determining the volume ratio of the pipette over the tank (Fig. 7). The standard deviation of the 10 GL-O pipette calibration points from the exponential fit of the ^{40}Ar decrease is of 0.6% (Fig. 7), comparable to the internal uncertainty of other laboratories [19]. The inter-laboratory uncertainty of the ^{40}Ar* content of the GL-O is the major limitation for the absolute calibration of our system sensitivity (i.e., 1% at the 1σ level [19]).

The accuracy of the calibrated system was tested against international K–Ar standards with various mineral phases used for the ^{40}Ar/^{39}Ar technique as neutron fluence monitors. These results are shown in Table 1 and represent a first and preliminary cross-calibration of several of these standards using the GL-O and the instrument presented here.

The MMhb-1 hornblende originates from a syenite of the McClure Mountain, Colorado, U.S.A. [20]. It is a widely used K–Ar standard and neutron fluence monitor, having a ^{40}Ar* content of $9.80 \pm 0.03 \times 10^{14}$ at./g for a reference age of 520.4 ± 1.7 Ma [21]. Later revisions proposed slightly older ages of 523.1 ± 2.6 or 525.1 ± 2.3 Ma, depending on the primary standard used [22], and 523.2 ± 0.9 Ma [19]. On a single measurement only, we obtained an ^{40}Ar* content of $10.03 \pm 0.1 \times 10^{14}$ at./g, which yields an age of 529.7 ± 7.2 Ma using the reference K content of 1.555 wt.% [21]. Within uncertainty, it is in agreement with reference ages listed above, as well as with the weighted mean of 525.0 ± 2.1 Ma [6] derived from nine replicate analyses performed in our laboratory using the Cassignol–Gillot technique relative to GL-O at 95.0 Ma [19].

The LP-6 biotite was extracted from a pyroxenite in the vicinity of the Similkameen pluton in Washington State, U.S.A. [20]. Its reference ^{40}Ar* content is $11.58 \pm 0.0062 \times 10^{14}$ at./g [19], with an age of 127.8 ± 0.7 Ma, which has been confirmed by more recent determinations of 128.1 Ma [21] and 127.5 ± 0.3 Ma [19]. We obtained three consistent ^{40}Ar* values of 11.76, 11.78 and $11.83 \pm 0.1 \times 10^{14}$ at./g defining a mean ^{40}Ar* content of 11.79 ± 0.1 at./g. Using the reference K value of 8.37 ± 0.05 wt.% [19], the weighted mean age is 130.1 ± 1.0 Ma, but we consider a 1% uncertainty as a minimum reasonable value, which yields an age of 130.1 ± 1.3 for LP-6 (Table 1). Both ages determined here for LP-6 and MMhb-1 are in agreement with their reference values within the 1% uncertainties, although we note that our ages are both on the older bounds of these intervals (Fig. 8). These results are similar to those obtained by cross-calibration of some standards against the GL-O [23], where ^{40}Ar* contents for LP-6 and MMhb-1 were higher than reference values. Note that in order to account for the inhomogeneity reported for both LP-6 and MMhb-1 at the mg level [24,25], we have used aliquots between 48 and 135 mg for the former, and about 30 mg for the latter (Table 1).

The TCR-2 sanidine was extracted from the Taylor Creek Rhyolite, New Mexico, U.S.A. and was proposed with a ^{40}Ar/^{39}Ar reference age of 27.92 ± 0.04 Ma, based on the SB-3 primary standard [26]. We have determined a K content of 7.055 ± 0.07 wt.% and a ^{40}Ar* content of $2.164 \pm 0.02 \times 10^{14}$ at./g, yielding an age of 29.13 ± 0.40 Ma, in agreement at the 2σ level with the revised reference age of 28.34 ± 0.16 Ma [22], and almost at the 1σ level, when a 1% uncertainty is considered for the reference age.

The RAC-20 sanidine of the Alder Creek Rhyolite in the Geyser–Cobb Mountain system, California, U.S.A., was pro-

posed as a Quaternary standard with the particularity of being the type occurrence of the Cobb mountain paleomagnetic excursion [27]. A mean age of 1.193 ± 0.001 Ma relative to FCs (28.02 Ma [22]) was recently proposed [28]. We obtained a K content of 8.84 ± 0.09 wt.% and a $^{40}Ar^*$ yield of $1.098 \pm 0.01 \times 10^{13}$ at./g giving an age of 1.189 ± 0.022 Ma (Table 1).

Finally, RMF96 sanidine, the youngest of the standards investigated here, was extracted from the White Trachytic Tuff of Roccamonfina volcano in Southern Italy [29] and has been proposed as a Plio-Pleistocene standard [30]. The reference age of the RMF96 sanidine was established by the K–Ar technique with a mean value of 0.331 ± 0.002 Ma and supported by $^{40}Ar/^{39}Ar$ analyses performed in two distinct laboratories [30]. We obtained here a single age determination of 0.340 ± 0.006 Ma (Table 1). The low radiogenic contents of 16 and 18% obtained for RAC-20 sanidine and RMF96 sanidine, respectively, are due to anomalously high hot blank levels. However, the correct age determinations demonstrate the adequacy of our atmospheric contamination correction. Accurate dating of standards (Fig. 8) with various mineralogies and radiogenic contents attests to the good behavior of the extraction–purification line and to the overall stability of the QMS.

4. Conclusions and perspectives

The performances of the standard resolution ion analyzer and of the electron multiplier of our QMS were optimized to provide stable mass filtering conditions and ion detection. The isotopic measurement procedure in routine analysis does not exceed 500 s and the high system sensitivity enables to deal with Ar quantities in the 10^{-12} to 10^{-9} mole range.

The $^{40}Ar/^{36}Ar$ ratio of the atmospheric standard is determined with a 0.05% accuracy and a 0.1% uncertainty, while the ^{40}Ar calibration of the QMS sensitivity is achieved with a 0.6% uncertainty using the GL-O international K–Ar standard. The latter uncertainty is likely bound to external variables such as weighting and heterogeneity of the standard material used for calibration. The absolute calibration of our system is therefore limited by such factors and the uncertainty on the determination of the absolute $^{40}Ar^*$ content of the standard itself, which is about 1%. The performances of the QMS–EM itself are, therefore, not the limiting factor for the accuracy of ^{40}Ar quantification. It is important to note that since the Cassignol–Gillot technique followed here relies on the direct comparison between the sample to be dated and aliquots of atmospheric argon, no assumption regarding the reference $^{40}Ar/^{36}Ar$ ratio of air is needed.

Geochronological standards MMhb-1 (520.4 ± 1.7 Ma, hornblende), LP-6 (127.8 ± 1.4 Ma, biotite), Taylor Creek Rhyolite (TCR; 27.92 ± 0.04 Ma, sanidine), Alder Creek Rhyolite (RAC-20; 1.193 ± 0.001, sanidine) and RMF96 (0.331 ± 0.002 Ma, sanidine) were dated at 529.7 ± 7.2, 130.1 ± 1.0, 29.13 ± 0.4, 1.189 ± 0.022 and 0.340 ± 0.006 Ma, respectively, consistent at the 1 or 2σ level with their published reference ages, and with more recent determinations as detailed above [18–29]. However, it can be noted that most ages obtained here (Table 1) are towards the older limit of the age standards and their uncertainties (Fig. 8), which can be due to either an uncorrected systematic error in our instrument, or a cross-calibration of GL-O with other standards which would require revision. In any case, these results demonstrate the ability of our QMS-based system for dating samples as young as Quaternary by the K–Ar technique, with 1σ total uncertainties for single determinations on the order of 1.4%, which is similar to that obtained by conventional magnetic sector mass spectrometers. Most of the results presented here were obtained from single analyses, and their analytical uncertainties can easily be reduced statistically by repeated measurements. However, it would be meaningless to provide any absolute age determination with a relative uncertainty lower than 1%, the reasonable uncertainty attached to the absolute age of standards used for calibration of the ^{40}Ar signal.

In the near future, a QMS will be used with a fully automated Ar processing high-vacuum line based on both a conventional RF furnace and a CO_2 laser total fusion extraction unit. Such a development aims at dating quantities of rock material more than one order of magnitude lower than what is conventionally used today, and with a greater productivity. This new line will also allow us to test this QMS for $^{40}Ar/^{39}Ar$ dating.

Acknowledgments

The authors wish to thank D.L. Pinti for having built the first version of the extraction–purification line and for providing constructive comments during the preparation of this manuscript. F. Elie is thanked for his precious assistance in the manufacturing of UHV line parts and M. Dumont for preparing glassware. Final comments by P. Sarda are appreciated. B. Orberger, P. Lahitte, A. Hildenbrand, M. Massault, R. Visocekas and A. Raquin are thanked for their support and assistance throughout the development of the analytical system. Jörg Pfänder and an anonymous reviewer are acknowledged for their helpful comments. This is LGMT contribution no. 70.

References

[1] C. Cassignol, P.-Y. Gillot, Range and Effectiveness of Unspiked Potassium–Argon Dating: Experimental Groundwork and Applications, John Wiley, New York, 1982.
[2] P.-Y. Gillot, Y. Cornette, Chem. Geol. 59 (1986) 205.
[3] E. Coulié, X. Quidelleur, J.C. Lefevre, P.Y. Gillot, Geochem. Geophys. Geosys. 5 (2004).
[4] E. Coulié, X. Quidelleur, P.-Y. Gillot, V. Courtillot, J.-C. Levèvre, S. Chiesa, Earth Planet. Sci. Lett. 206 (2003) 477.
[5] A. Hildenbrand, P.-Y. Gillot, I. Le Roy, Earth Planet. Sci. Lett. 217 (2004) 349–365.
[6] N. Fiet, X. Quidelleur, O. Parize, L.-G. Bulot, P.-Y. Gillot, EPSL 246 (2006) 407.
[7] A.L. Chenet, X. Quidelleur, F. Fluteau, V. Courtillot, S. Bajpai, EPSL 263 (2007) 1.
[8] A. Samper, X. Quidelleur, P. Lahitte, D. Mollex, Earth Planet. Sci. Lett. 258 (2007) 175.
[9] X. Quidelleur, P.Y. Gillot, V. Soler, J.C. Lefèvre, Geophys. Res. Lett. 28 (2001) 3067.
[10] I. McDougall, T.M. Harrison, Geochronology and Thermochronology by the $^{40}Ar/^{39}Ar$ Method, Oxford University Press, New York, 1999.
[11] K. Hashizume, N. Sugiura, Mass Spectrosc. 38 (1990) 269.
[12] J.T. Kulongoski, D.R. Hilton, Geochem. Geophys. Geosyst. 3 (2002) U1.

[13] Y. Sano, N. Takahata, J. Oceanogr. 61 (2005) 465.
[14] B. Marty, M. Lenoble, N. Vassard, Chem. Geol. 120 (1995) 183–195.
[15] T. Yamamoto, K. Hashizume, J. Matsuda, T. Kase, Meteorit. Planet. Sci. 33 (1998) 857.
[16] R. Hamme, S.R. Emerson, Mar. Chem. 91 (2004) 53.
[17] D.L. Pinti, K. Hashizume, J. Matsuda, Geochim. Et Cosmochim. Acta 65 (2001) 2301.
[18] R.H. Steiger, E. Jäger, Earth Planet. Sci. Lett. 36 (1977) 359.
[19] G.S. Odin, in: G.S. Odin (Ed.), Interlaboratory Standards for Dating Purposes, John Wiley and Sons, Chichester, 1982, p. 123.
[20] E.C. Alexander, G.M. Mickelson, M.A. Lanphere, U.S. Geol. Surv., Open File Report 78, 1978, 6.
[21] S.D. Samson, E.C.J. Alexander, Chem. Geol. 66 (1987) 27.
[22] P.R. Renne, C.C. Swisher, A.L. Deino, D.B. Karner, T.L. Owens, D.J. DePaolo, Chem. Geol. 145 (1998) 117.
[23] S. Charbit, H. Guillou, L. Turpin, Chem. Geol. 150 (1998) 147.
[24] T.L. Spell, I. McDougall, Chem. Geol. 198 (2003) 189.
[25] A.K. Baksi, D.A. Archibald, E. Farrar, Chem. Geol. 129 (1996) 307.
[26] W.A. Duffield, G.B. Dalrymple, Bull. Volcanol. 52 (1990) 475.
[27] B.D. Turrin, J.M. Donnelly-Nolan, B.J. Carter Hearn, Geology 22 (1994) 251.
[28] S. Nomade, P.R. Renne, N. Vogel, A.L. Deino, W.D. Sharp, T.A. Becker, A.R. Jaouni, R. Mundil, Chem. Geol. 218 (2005) 315.
[29] V. Rouchon, P.-Y. Gillot, X. Quidelleur, S. Chiesa, B. Floris, J. Volcanol. Geothermal Res., submitted for publication.
[30] X. Quidelleur, P.-Y. Gillot, M. Grove, T.M. Harrison, A. Deino, The White Trachytic Tuff sanidine: a potential age standard for $^{40}Ar/^{39}Ar$ dating of Pleistocene-Pliocene samples, in: Terra Cognita 9, 1997, p. 69.
[31] J.R. Taylor, An Introduction to Error Analysis, University Science Books, Mill Valley, 1982.